UDK 661.665.3620.18
Original scientific article/Izvirni znanstveni članek

ISSN 1580-2949
MTAEC9, 56(3)263(2022)

INFLUENCES OF BORON CARBIDE PARTICLES ON THE WEAR RATE AND TENSILE STRENGTH OF AA2014 SURFACE COMPOSITE FABRICATED BY FRICTION-STIR PROCESSING

VPLIV BOR-KARBIDNIH DELCEV NA HITROST OBRABE POVRŠINE IN NATEZNO TRDNOST KOMPOZITA VRSTE AA2014, IZDELANEGA S PROCESOM TORNEGA GNETENJA

Sampath Boopathi[1*], V. Haribalaji[2], M. Mageswari[3], M. Mohammed Asif[4]

[1]Department of Mechanical Engineering, Muthayammal Engineering College, Namakkal, Tamil Nadu, India, 637 408
[2]Department of Mechanical Engineering, Narasu's Sarathy Institute of Technology, Salem, Tamil Nadu, India, 636 305
[3]Department of Civil Engineering, Panimalar Engineering College, Chennai, Tamil Nadu, India, 600123
[4]Department of Mechanical Engineering, Vignan's Lara Institute of Technology and Science, Guntur, Andra Pradesh, India, 522213

Prejem rokopisa – received: 2022-02-16; sprejem za objavo – accepted for publication: 2022-03-24

doi:10.17222/mit.2022.409

In this article, a boron carbide particle (B_4C) reinforced AA2014 surface composite was first fabricated by friction-stir processing (FSP) to investigate the impact of the volume percentage of B_4C, tool rotational speed and table speed on the tensile strength (TS) and wear rate (WR). The AA2014 composite is one of the important candidates for making defense and aerospace components due to its high strength and minimum weight. Taguchi orthogonal array was employed to design and predict the maximum tensile strength and minimum wear rate. The volume percentage of B_4C is the most momentous parameter for both the tensile strength and wear rate. The optimum parameter settings for attaining the maximum tensile strength of 605 MPa and a minimum wear rate of 1.2 mm^3/Nm are a B_4C volume of 15 %, tool rotational speed of 900 min^{-1} and table speed of 60 mm/min. The optimum process-parameter settings were used to make a specimen for validating the estimated results. The microstructure and chemical composition of the surface composite of the optimum specimen were illustrated using scanning electron microscopy (SEM) and energy-dispersive X-ray spectroscopy (EDS), respectively. The surface profile and microscopic view of the worn-out surface composite were also examined using SEM images.

Keywords: boran carbide, microstructure, tensile strength, wear characteristics

V tem članku avtorji opisujejo najprej izdelavo kompozitne površine Al zlitine AA2014 ojačane z bor-karbidnimi delci (B_4C) s pomočjo procesa tornega gnetenja (angl.: FSP; friction-stir process) in nato raziskavo vpliva volumskega deleža dodanih B_4C delcev, hitrosti vrtenja in potovanja orodja na natezno trdnost (TS) in hitrost obrabe (WR) izdelane kompozitne površine. Aluminijeva zlitina AA2014 je ena od najpomembnejših kandidatk za uporabo pri izdelavi komponent vojaške in letalske industrije zaradi visoke trdnosti na enoto specifične gostote zlitine (MP/(kg·m^3)). Avtorji so uporabili Taguchijevo ortogonalno matrico za dizajn in napoved maksimalne TS in minimalne WR. Ugotovili so, da je najbolj pomemben parameter volumski delež B_4C, ki vpliva tako na TS, kot tudi WR. Ugotovili so tudi, da so bili izbrani parametri procesa optimalni pri 15 % volumskem deležu B_4C, hitrosti vrtenja orodja 900 min^{-1} in njegovi hitrosti pomika oz. pomika mize 60 mm/min. Pri tem je bila dosežena natezna trdnost 605 MPa z najmanjšo hitrostjo obrabe 1,2 mm^3/(N·m). Za ovrednotenje eksperimentalnih rezultatov so bili izdelani ustrezni preizkušanci in izbrane ustrezne nastavitve izbranih procesnih parametrov. Mikrostrukture in kemijske sestave površin izdelanih kompozitov so v članku predstavljene s posnetki izdelanimi na vrstičnem elektronskem mikroskopu (SEM) in z energijsko disperzijsko spektroskopijo rentgenskih žarkov (EDXS). Prav tako so profile površin in makroskopske poglede obrabljenih površin kompozitov analizirali in predstavili s pomočjo SEM posnetkov.

Ključne besede: bor-karbid, mikrostruktura, natezna trdnost, obraba

1 INTRODUCTION

Friction-stir processing (FSP) is an eco-friendly surface-modification technique for making surface composites with a frictional and thermo-mechanical process to improve the grain size, surface texture, microhardness and tensile strength. In a previous research, a hard tool was rotated over soft-material surfaces with micro- or nanoparticles to obtain a surface composite.[1] This research on various FSP aluminium alloys and their surface composites was performed with FSP to improve their mechanical properties.

The hardness of an AA1050 surface composite was significantly improved by reinforcing it with micro-sized mixed Al_2O_3 and SiC particles. It was observed that the hardness was improved by three times when compared to the base alloy.[2,3] Similarly, the hardness of an AA2024 surface composite was significantly enhanced by infiltrating Al_2O_3 nanoparticles, using the moderate speed of a threaded cylindrical tool.[4] The wear rate and hardness of an AA5052-SiC surface composite were substantially improved by using 5-μm metal particles and the moderate speed of a square tool. The thermal conductivity of AA5052 alloys was improved by reinforcing them with micro-sized graphene particles with the moderate speed of a taper-shaped tool during FSP.[5] The hardness of an

*Corresponding author's e-mail:
boopasangee@gmail.com

AA5083 alloy was significantly enhanced by adding SiC and ZrO_2 powders to it using the friction-stir process.[6,7] The hardness and wear resistance of an AA6061 alloy surface was also increased by reinforcing it with a mixture of SiC and Al_2O_3 particles and the moderate speed of a threaded taper cylindrical tool.[8] After imposing the size of 60 μm of TiB_2 and 10 μm of SIC particles on an AA6063 alloy with FSP, using threaded cylindrical tools, the surface hardness was enhanced by 2.15 times.[9,10] The wear resistance of an AA7075 surface composite was improved by adding TiN and SiC particles with sizes of 45–60 nm at the high speed of a triangular-shaped tool in the groove slotted during FSP.[11,12] The hardness of carbon-nanotube (CNT) particles imposed on an AA7075 surface composite using the high speed of a cylindrical tool is more than two times higher than that of the base alloy.[13] The wear resistance of an AA6360 surface composite infiltrated by TiC and B_4C particles was improved by more than 1.5 times when using a threaded cylindrical tool in the groove slots.[14] An AA6082 surface composite was fabricated using a multi-pass threaded cylindrical tool during FSP to examine its microhardness and wear resistance. It was revealed that the wear rate was reduced by two times and the hardness was improved by 2.4 times when compared to the base alloy surface.[15] Thus, the square-shaped and threaded tools were widely applied to improve the grain refinement and microhardness of aluminium alloy surface composites. The triangular and square-shaped tools were also applied to increase the tensile strength and ductility of aluminium surface composites.[16,17]

An AA1050 hybrid composite was formed with FSP using Fe_2O_3 and aluminium-nanoparticle reinforcement to improve the hardness and tensile strength to the maximum level.[18] Similarly, the tensile strength and wear resistance of an AA5083 alloy were improved with a reinforcement with a mixture of Al_2O_3 (80 nm) and TiO_2 (15 nm) nanoparticles using the FSP method.[19] An AA5083 hybrid surface composite with SiC and Al_2O_3 micro-sized powders was fabricated with FSP to enhance the wear resistance and hardness.[20] The hardness and tensile strength were improved by adding carbon-nanotube (CNT) particles onto an AA5083 alloy using FSP.[21] An AA6061 surface composite was fabricated with FSP using the reinforcement of fine ceramic particles on the surface. The microhardness, wear-resistance and coefficient of friction of the surface were greatly enhanced by FSP.[22] An AA7075 alloy was reinforced with palm kernel shell ash particles via FSP to examine various mechanical properties. The tensile strength and wear resistance were increased by adding ash particles.[23] Very recently, the tensile strength and microhardness of an AA2024 alloy surface were improved using 1000 min^{-1} speed of the cylindrical tool during FSP.[24] Effects of the boron-carbide quantity, feed rate and tool speed on the tensile stress and wear resistance of an AA6061-B_4C surface composite were investigated with the Taguchi technique. It was revealed that the mechanical properties of the aluminium surface composite were significantly improved by adding B_4C.[25]

Thus, it was observed from the above literature that the mechanical properties of various aluminium surface composites were significantly improved with the reinforcement of various micro- and nano-sized metal particles using friction-stir processing. However, the AA2014-B_4C surface composite was never fabricated with FSP to investigate the influences of the process parameters on the tensile strength and wear rate. In this research, B_4C particles reinforced AA2014 alloy surfaces using friction-stir processing to examine the modifications of the tensile strength and wear resistance, using the Taguchi design of experimentation. The optimum FSP parameter setting was predicted to maximize the tensile strength and minimize the wear rate using the Taguchi technique.

2 EXPERIMENTAL PART

The FSP experimental set-up for fabricating an AA2014–B_4C surface composite is displayed in **Figure 1.** In this research, the dimensions of the AA2014 alloy are (0.1 × 0.05 × 0.008) m, selected on the basis of its use in defense, aerospace and various industrial applications due to its low weight and high strength.[26] The mechanical properties and various elements of AA2014 are illustrated in **Table 1**. The element composition of AA2014 was detected with ARL100 optical emission spectrometry. The B_4C powder with a mean grain size of 10 μm was selected for the surface reinforcement to increase the hardness and tensile strength. The volume percentage of B_4C was varied between (5, 10 and 15) φ/%. A groove with a width of 0.02 m was fabricated in the middle of the AA2014 plate. The volume of the groove was adjusted to the depth of the slot. A 65 HRC hardened H13 steel cylindrical rod with a 0.02 m shoulder diameter was used as the tool for FSP. The length and pin diameter of the tool were 0.004 m and 0.006 m, respectively. FSP was carried out using a CNC friction-stir-welding machine. The powder was heated and logged over the aluminium surface by a rotating tool. The tool rotating speed varied between (800, 900 and 1000) min^{-1}. The traveling speed of the table varied between (40, 50 and 60) mm/min.

The tensile and wear tests were performed, using the ASTM-E8 and ASTM G99-05 standards, via a wire electrical discharge process without damaging the surface. A pin-on-disc instrument was used to find the wear of the surface composite. The experiments were conducted at a sliding length of 1000 m, force of 30 N and rotational speed of 1500 min^{-1}. The wear rate was determined from the wear loss of each specimen using Equation (1).

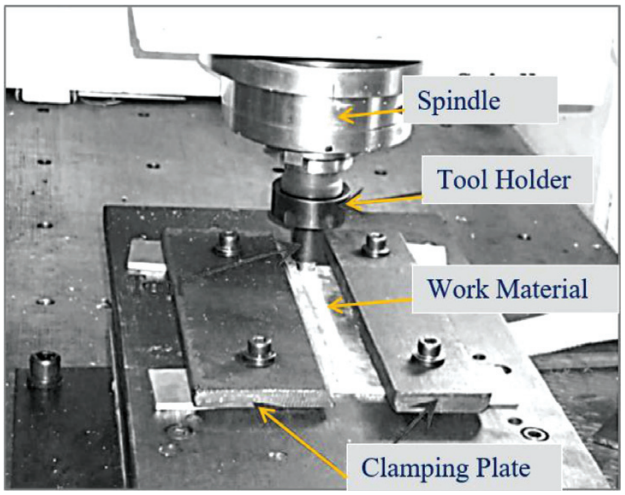

Figure 1: Friction-stir processing of AA2014 using B_4C

$$\text{Wear rate} = \frac{\text{wear loss}}{\text{density} \cdot \text{load} \cdot \text{sliding distance}} \quad (\text{mm}^3/(\text{N}\cdot\text{m})) \tag{1}$$

Table 1: Mechanical properties and chemical composition of AA2014

Parameter	Value
Specific heat (J/kg °C)	880
Thermal conductivity (W/mK)	154
palphaMelting point (°C)	638
Vickers hardness (HV)	155
Tensile strength (MPa)	470
Density (kg/m^3)	2800
Chemical elements (volume percentage)	Ti 0.02 %; Mn 0.58 %; Fe 0.223 %; Ni 0.019 %; Mg-0.358 %, Zn-0.199 %, Cu-4.64 %, Si-0.668 %, Al-93.24 %

Taguchi's L9 orthogonal array was selected for three level/three parameter welding. It is a simple fractional factorial design with a minimum number of experiments. Initially, the levels of each parameter were selected based on exploratory experiments and experts' suggestions. The values for each level of the selected process parameters are illustrated in **Table 2.** Three replications of nine experiments were performed to prepare the specimens and conduct the tensile and wear tests.[2] All the experiments were conducted randomly to avoid experimental error. After conducting the experiments, a total of 27 observations were noted in **Table 3**.

The Taguchi analysis was performed to find the impacts of the process parameters on the tensile strength and wear rate. MiniTab trial version software was used to determine the signal-to-noise ratio (*S*/*N*), percentage of contribution of each parameter and analysis of variance for the welding characteristics. Equations (2) and (3) were applied to calculate the S/N to maximize the tensile strength and minimize the wear rate. The S/N for the tensile strength and wear rate is shown in **Table 3.**

$$S/N \text{ for maximization: } \frac{S}{N_{\max}} = -10\lg\left(\frac{\sum_{p=1}^{k} TS_p^2}{p}\right) \tag{2}$$

$$S/N \text{ for minimization: } \frac{S}{N_{\min}} = -10\lg\left(\frac{\sum_{p=1}^{k} \frac{1}{WR_p^2}}{p}\right) \tag{3}$$

Here, $p = 3$ the number of replications, $K = 9$ is number experiments, WR_p – the wear rate response value of p^{th} experiment, TS_p – the tensile strength response value of p^{th} experiment.

The values for the tensile strength and wear rate obtained with Taguchi's analysis are shown in **Table 4**. The percentage of contribution of each parameter was calculated with the ratio of the sequential sum of squares and the total sequential sum of squares for each response us-

Table 2: Volume percentage of B_4C, tool speed and table speed for the FSP experimentation

Level	Notation	Low	Medium	High
Volume percentage of B_4C (φ/%)	P	5	10	15
Tool rotating speed (min^{-1})	N	800	900	1000
Table speed (mm/min)	T	50	60	70

Table 3: FSP experimental observations and S/N values

Exp. No.	P	N	T	Tensile strength					Wear rate				
				Trail 1	Trail 2	Trail 3	Mean	S/N	Trail 1	Trail 2	Trail 3	Mean	S/N
1.	5	800	50	496.99	496.15	497.02	496.72	53.92	1.99	1.89	1.97	1.95	–5.80
2.	5	900	60	545.67	544.66	545.58	545.30	54.73	1.55	1.54	1.51	1.53	–3.71
3.	5	1000	70	529.33	528.44	529.74	529.17	54.47	1.71	1.68	1.72	1.70	–4.63
4.	10	800	60	556.75	555.53	556.89	556.39	54.91	1.74	1.77	1.78	1.76	–4.93
5.	10	900	70	572.95	572.06	572.69	572.57	55.16	1.49	1.45	1.50	1.48	–3.41
6.	10	1000	50	538.28	537.21	538.32	537.94	54.61	1.68	1.66	1.70	1.68	–4.51
7.	15	800	70	577.17	576.53	577.67	577.12	55.23	1.55	1.53	1.52	1.53	–3.71
8.	15	900	50	575.33	574.19	575.37	574.96	55.19	1.31	1.32	1.31	1.31	–2.37
9.	15	1000	60	595.14	594.01	595.09	594.75	55.49	1.34	1.36	1.34	1.35	–2.59

Table 4: Tensile strength and wear rate analysis using experimental data

Source	Degree of freedom	Sequential sum of squares	Variance	Percentage of contribution (%)
Tensile strength				
Volume percentage of B_4C	2	5155.37	2577.68	71.44
Table speed	2	653.15	326.57	9.05
Tool speed	2	1404.55	702.27	19.46
Error	2	2.87	1.43	0.04
Total	8	7215.93	–	100
Wear rate				
Volume percentage of B_4C	2	0.1766	0.0883	52.72
Table speed	2	0.1418	0.0709	42.34
Tool speed	2	0.0163	0.0082	4.87
Error	2	0.0002	0.0001	0.07
Total	8	0.3348	–	100

ing experimental data. The effects of the signal-to-noise ratio, mean and standard deviation values of the process parameters on maximizing the tensile strength are illustrated in **Figure 2**. Similarly, the effects of the signal-to-noise ratio, mean and standard deviation values of the process parameters on minimizing the wear rate are illustrated in **Figure 3**. The signal-to-noise ratio was used to convert different ranges of responses to normalized values for easy calculation. The standard deviation was used to examine the variations in the response values due to the noises during the experimentations.

3 RESULTS AND DISCUSSIONS

As per the Taguchi Analysis, the percentage of the B_4C contribution to the tensile strength was 71.44 % and for the wear rate, it was 52.72 % due to a proper reinforcement of B_4C particles of the AA2014 surfaces. When increasing the volume percentage of B_4C, the tensile strength was enhanced due to the reinforcement and

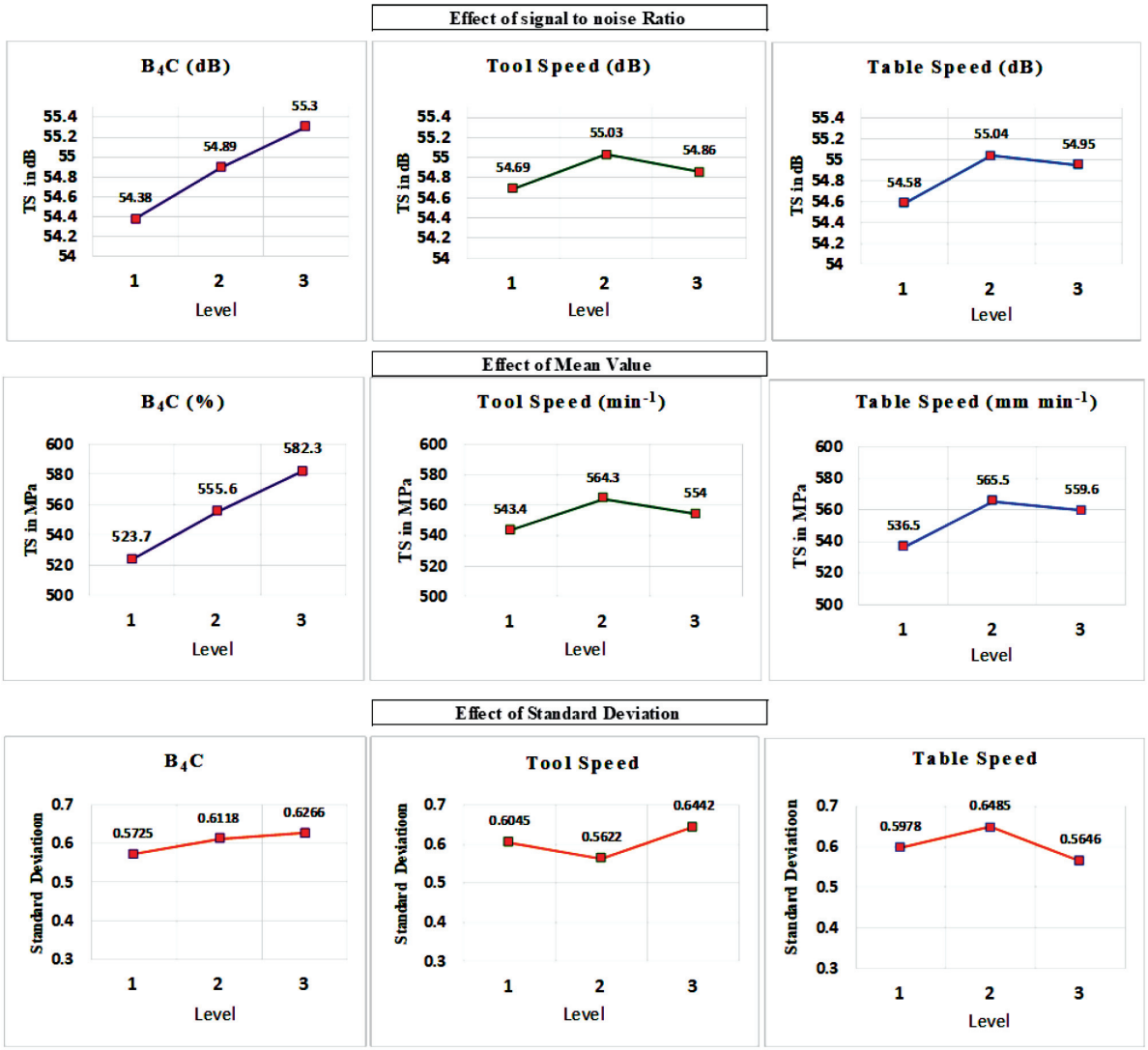

Figure 2: Effects of signal-to-noise ratio, mean and standard deviation of process parameters on the tensile strength

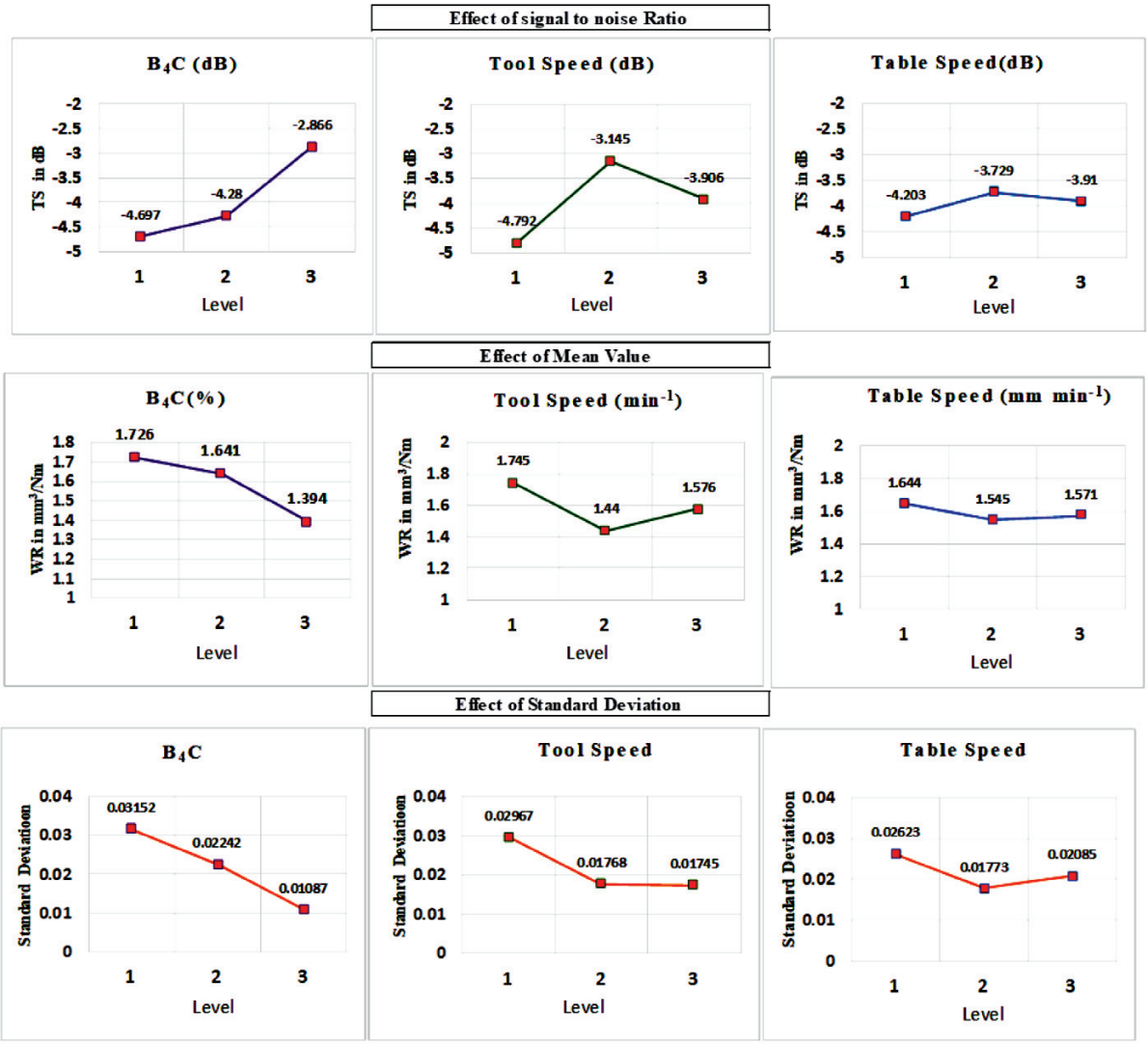

Figure 3: Effects of signal-to-noise ratio, mean and standard deviation of process parameters on the wear rate

infiltration of B_4C particles onto the base metal surfaces. Moderate tool rotational speed (Level 2) and table traveling speed (Level 2) are selected as the optimum setting for the highest tensile strength.

The percentage of the contribution of the tool rotational speed to the tensile strength and wear rate was 9.05 % and 42.34 %, respectively. When increasing the tool speed above Level 2, the tensile strength and wear rate were minimized by improper distributions of the B_4C particles on the hot surfaces. Improper distribution occurred due to the peak temperature reaching the ultimate level in the friction-stir-zone.

When enhancing the table traveling speed up to Level 2, the tensile strength was increased and the wear rate was decreased due to the uniform reinforcement of B_4C particles on the alloy surfaces. After further increasing the table traveling speed, both responses deviated from their optimum values due to a discrete reinforcement of B_4C particles on the aluminium alloy surfaces caused by the high table speed affecting the rotating tool.

Thus, the third level of B_4C (15 %), the second level of the tool rotational speed (900 min^{-1}) and the second level of the table speed (60 mm/min) were predicted as the optimum process parameters for maximizing the tensile strength (604.276 MPa) and minimizing the wear rate (1.21 $mm^3/(N{\cdot}m)$) of the AA2014-B_4C surface composite. These settings were validated with confirmation experiments. An FSP specimen was prepared using the

Table 5: Estimated optimum values and confirmation-test results

Characteristics	Predicted value	Experimental value	Parameters		
			B_4C (φ/%)	Table speed (mm/min)	Tool rotational speed (min^{-1})
Tensile strength (MPa)	604.276	605	15	60	900
Wear rate ($mm^3/(N{\cdot}m)$)	1.21	1.2			

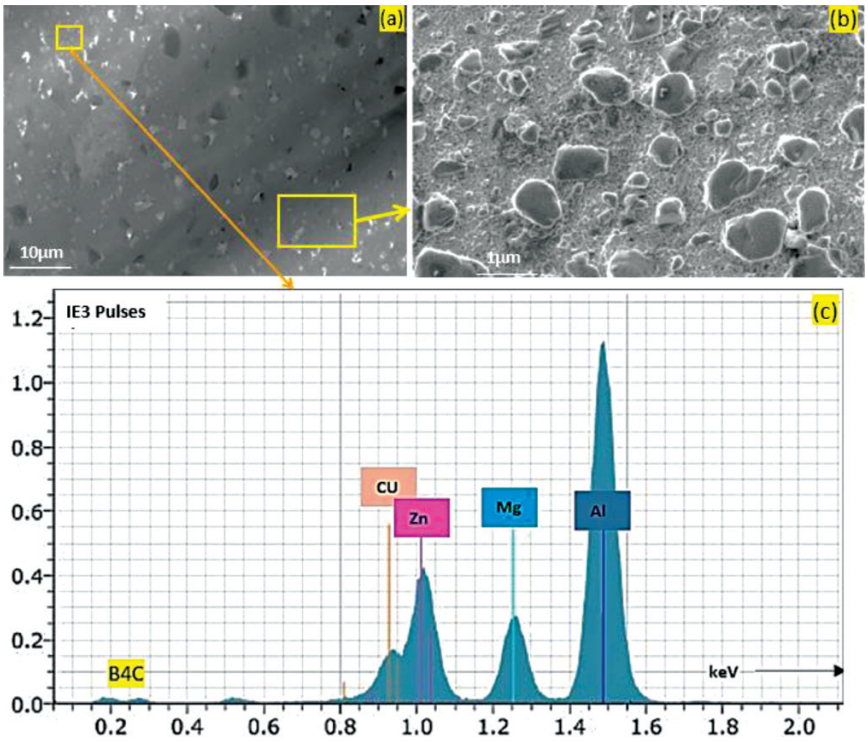

Figure 4: a) SEM image of AA2014-B_4C surface composite, b) TEM image of AA2014-B_4C surface composite at the selected spot, c) EDS image of the surface composite at the selected spot

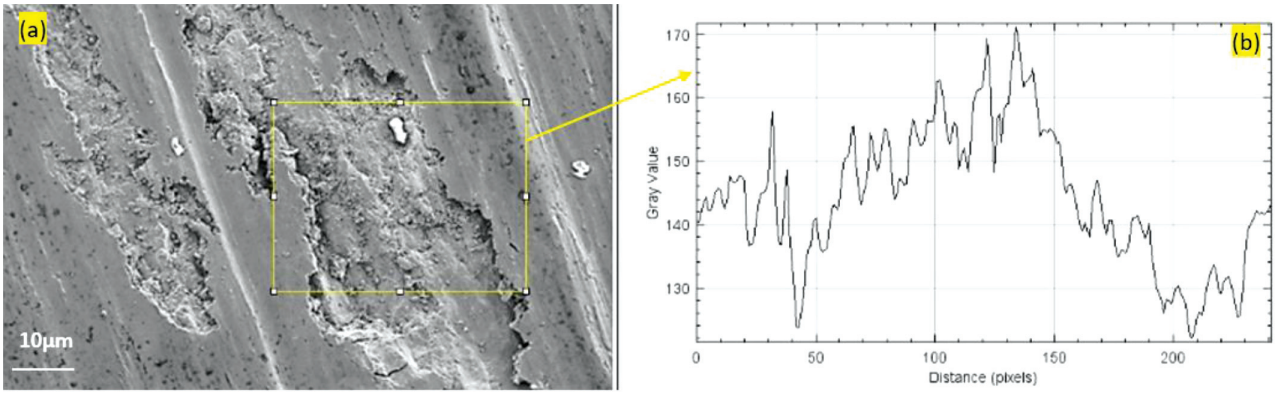

Figure 5: Optimum specimen worn-out surface: a) SEM image of surface, b) profile during the wear test

optimum settings, and tensile and wear tests were carried out using the same procedure. The results predicted with the Taguchi method and confirmation-test results were compared as shown in **Table 5**. The optimum settings for the specimen were used to examine the microstructure and perform an EDS analysis.

A SEM image of the AA2014-B_4C surface is shown in **Figure 4a**. A uniform distribution of B_4C particles was observed on the composite surfaces. It was also validated with a transmission electron microscope (TEM) image shown in **Figure 4b**. The various elements of the AA2014-B_4C composite surface are illustrated in the 0.2 keV scale of the EDS plot, as shown in **Figure 4c**. The major metallic elements, (Al 90.31; Cu 4.76; B 1.82; C 0.84; Fe 0.23; Mn 0.51; Zn 0.43; Si 0.78; Mg 0.32) *w*/% on the surface composite, are examined with an EDS analysis. A microstructural view of the worn-out surface of the optimum specimen and its surface profile after the wear test are illustrated in **Figures 5a** and **5b**, respectively. It is observed from the profile plot that the grayscale distribution is between gray values of 120 and 171 with respect to the pixel levels. Grayscale is used to indicate the depth of the worn-out surface.

4 CONCLUSIONS

In this research, an AA2014-B_4C surface composite was prepared using FSP to improve the tensile strength and minimize the wear rate. It was revealed from the

Taguchi analysis that the volume percentage of B_4C significantly affected both the tensile strength and wear rate of the surface composite. It was observed that a uniform distribution of the reinforcing B_4C particles on the base AA2014 alloy was obtained through FSP. The maximum tensile strength (605 MPa) and minimum wear rate (1.2 $mm^3/(N{\cdot}m)$) of the surface composite were obtained with a combination of the optimum process parameters: a B_4C of 15 φ/%, tool rotational speed of 900 min^{-1} and table speed of 60 mm/min. The microstructure, distribution of various metallic elements, and B_4C particle distribution in the AA2014 surface composite were determined with SEM, EDS and TEM analyses, respectively. The microstructure and surface profile of a worn-out surface composite were also illustrated.

Acknowledgements

The authors would like to thank the Center of Composite Materials at Salem Material Technology and Company (SMT), Tamil Nadu, India, for conducting the tests and analysing the results.

5 REFERENCES

[1] M. Sharifitabar, M. Kashefi, S. Khorshahian, Effect of friction stir processing pass sequence on properties of Mg-$ZrSiO_4$-Al_2O_3 surface hybrid micro/nano-composites, Materials and Design, 108 (**2016**) 1–7, doi:10.1016/j.matdes.2016.06.087

[2] A. Kurt, I. Uygur, E. Cete, Surface modification of aluminium by friction stir processing, Journal of Materials Processing Technology, 211 (**2011**) 3, 313–317, doi:10.1016/j.jmatprotec.2010.09.020

[3] E. R. I. Mahmoud, M. Takahashi, T. Shibayanagi, K. Ikeuchi, Wear characteristics of surface-hybrid-MMCs layer fabricated on aluminum plate by friction stir processing, Wear, 268 (**2010**) 9–10, 1111–1121, doi:10.1016/j.wear.2010.01.005

[4] B. Zahmatkesh, M. H. Enayati, A novel approach for development of surface nanocomposite by friction stir processing, Materials Science and Engineering A, 527 (**2010**) 24–25, 6734–6740, doi:10.1016/j.msea.2010.07.024

[5] C. H. Jeon, Y. H. Jeong, J. J. Seo, H. N. Tien, S. T. Hong, Y. J. Yum, S. H. Hur, K. J. Lee, Material properties of graphene/aluminum metal matrix composites fabricated by friction stir processing, International Journal of Precision Engineering and Manufacturing, 15 (**2014**) 6, 1235–1239, doi:10.1007/s12541-014-0462-2

[6] V. Sharma, Y. Gupta, B. V. M. Kumar, U. Prakash, Friction Stir Processing Strategies for Uniform Distribution of Reinforcement in a Surface Composite, Materials and Manufacturing Processes, 31 (**2016**) 10, 1384–1392, doi:10.1080/10426914.2015.1103869

[7] S. Shahraki, S. Khorasani, R. Abdi Behnagh, Y. Fotouhi, H. Bisadi, Producing of AA5083/ZrO_2 nanocomposite by friction stir processing (FSP), Metallurgical and Materials Transactions B: Process Metallurgy and Materials Processing Science, 44 (**2013**) 6, 1546–1553, doi:10.1007/s11663-013-9914-9

[8] A. Devaraju, A. Kumar, B. Kotiveerachari, Influence of rotational speed and reinforcements on wear and mechanical properties of aluminum hybrid composites via friction stir processing, Materials and Design, 45 (**2013**), 576–585, doi:10.1016/j.matdes.2012.09.036

[9] M. Narimani, B. Lotfi, Z. Sadeghian, Investigating the microstructure and mechanical properties of Al-TiB2 composite fabricated by Friction Stir Processing (FSP), Materials Science and Engineering A, 673 (**2016**), 436–442, doi:10.1016/j.msea.2016.07.086

[10] S. Rathee, S. Maheshwari, A. N. Siddiquee, M. Srivastava, Investigating Effects of Groove Dimensions on Microstructure and Mechanical Properties of AA6063/SiC Surface Composites Produced by Friction Stir Processing, Transactions of the Indian Institute of Metals, 70 (**2017**) 3, 809–816, doi:10.1007/s12666-017-1060-7

[11] M. Bahrami, M. K. Besharati Givi, K. Dehghani, N. Parvin, On the role of pin geometry in microstructure and mechanical properties of AA7075/SiC nano-composite fabricated by friction stir welding technique, Materials and Design, 53 (**2014**), 519–527, doi:10.1016/j.matdes.2013.07.049

[12] S. F. Kashani-Bozorg, K. Jazayeri, Formation of Al/B4C surface nano-composite layers on 7075 Al alloy employing friction stir processing, AIP Conference Proceedings, 1136 (**2009**) 2009, 715–719, doi:10.1063/1.3160241

[13] D. K. Lim, T. Shibayanagi, A. P. Gerlich, Synthesis of multi-walled CNT reinforced aluminium alloy composite via friction stir processing, Materials Science and Engineering A, 507 (**2009**) 1–2, 194–199, doi:10.1016/j.msea.2008.11.067

[14] C. M. Rejil, I. Dinaharan, S. J. Vijay, N. Murugan, Microstructure and sliding wear behavior of AA6360/(TiC+B 4C) hybrid surface composite layer synthesized by friction stir processing on aluminum substrate, Materials Science and Engineering A, 552 (**2012**), 336–344, doi:10.1016/j.msea.2012.05.049

[15] A. Shafiei-Zarghani, S. F. Kashani-Bozorg, A. Zarei-Hanzaki, Microstructures and mechanical properties of Al/Al2O3 surface nano-composite layer produced by friction stir processing, Materials Science and Engineering A, 500 (**2009**) 1–2, 84–91, doi:10.1016/j.msea.2008.09.064

[16] G. Hussain, R. Hashemi, H. Hashemi, K. A. Al-Ghamdi, An experimental study on multi-pass friction stir processing of Al/TiN composite: some microstructural, mechanical, and wear characteristics, International Journal of Advanced Manufacturing Technology, 84 (**2016**) 1–4, 533–546, doi:10.1007/s00170-015-7504-5

[17] K. Elangovan, V. Balasubramanian, M. Valliappan, Influences of tool pin profile and axial force on the formation of friction stir processing zone in AA6061 aluminium alloy, International Journal of Advanced Manufacturing Technology, 38 (**2008**) 3–4, 285–295, doi:10.1007/s00170-007-1100-2

[18] N. A. Patil, S. R. Pedapati, O. Bin Mamat, A review on aluminium hybrid surface composite fabrication using Friction Stir Processing, Archives of Metallurgy and Materials, 65 (**2020**) 1, 441–457, doi:10.24425/amm.2020.131747

[19] A. Heidarpour, S. Ahmadifard, S. Kazemi, On the Al5083–Al2O3–TiO2 Hybrid Surface Nanocomposite Produced by Friction Stir Processing, Protection of Metals and Physical Chemistry of Surfaces, 54 (**2018**) 3, 409–415, doi:10.1134/S2070205118030279

[20] E. M. Zayed, N. S. M. El-Tayeb, M. M. Z. Ahmed, R. M. Rashad, Development and characterization of AA5083 reinforced with SiC and Al2O3 particles by friction stir processing, Advanced Structured Materials, 92 (**2019**), doi:10.1007/978-3-319-79005-3_2

[21] R. Raja, S. Jannet, S. R. Ruban, Mechanical and metallurgical studies of multi-walled carbon nanotube– reinforced aluminium metal matrix surface composite by friction stir processing, International Journal of Advanced Technology and Engineering Exploration, 8 (**2021**) 78, 643–650, doi:10.19101/IJATEE.2021.874038

[22] V. P. Kushwaha, S. Joshi, R. C. Singh, R. Chaudhary, Characterisation of floor tiles reinforced aluminium surface composite synthesized by friction stir processing, IOP Conference Series: Materials Science and Engineering, 804 (**2020**) 1, doi:10.1088/1757-899X/804/1/012013

[23] O. M. Ikumapayi, E. T. Akinlabi, J. D. Majumdar, S. A. Akinlabi, Characterization of high strength aluminium-based surface matrix composite reinforced with low-cost PKSA fabricated by friction stir processing, Materials Research Express, 6 (**2019**) 10, doi:10.1088/2053-1591/ab395b

[24] S. Boopathi, M. Jeyakumar, G. R. Singh, F. L. King, M. Pandian, R. Subbiah, V. Haribalaji, An experimental study on friction stir pro-

cessing of aluminium alloy (AA-2024) and boron nitride (BNp) surface composite, Materials Today: Proceedings, (**2022**), doi:10.1016/j.matpr.2022.02.435

[25] S. Boopathi, A. Thillaivanan, M. Pandian, R. Subbiah, P. Shanmugam, Friction stir processing of boron carbide reinforced aluminium surface (Al-B_4C) composite: Mechanical characteristics analysis, Materials Today: Proceedings, 50 (**2022**), 2430–2435, doi:10.1016/j.matpr.2021.10.261

[26] R. Kadaganchi, M. R. Gankidi, H. Gokhale, Optimization of process parameters of aluminum alloy AA 2014-T6 friction stir welds by response surface methodology, Defence Technology, 11 (**2015**) 3, 209–219, doi:10.1016/j.dt.2015.03.003